GEOMORPHOLOGY

ELSEVIER

Acceleration of Horton overland flow and erosion by footpaths in an upland agricultural watershed in northern Thailand

A.D. Ziegler [a,b,*], R.A. Sutherland [b], T.W. Giambelluca [b]

[a] *Water Resources Program, EEWR, E-Quad, E-228, Princeton University, Princeton, NJ 08544, USA*
[b] *Geography Department, University of Hawaii, 2424 Maile Way, Honolulu, HI 96822, USA*

Abstract

Through field rainfall simulation experiments in an upland mountainous watershed of northern Thailand, we have identified two phenomena that increase the potential for Horton overland flow (HOF) generation on agricultural lands. First, there appears to be a transition period of 12–18 months, extending from the time of abandonment until the formation of a dense vegetation layer capable of intercepting rainfall and ponding surface water, during which HOF generation is accelerated. Simulation data indicate these recently abandoned fields may have runoff coefficients (ROCs) as high as 40% during large seasonal storms with wet antecedent soil moisture conditions. In comparison, actively cultivated lands and advanced (> 16–18 months) fallow fields, the land surfaces existing before and after the threshold period, have ROCs $\leq 4\%$. Secondly, compacted path surfaces initiate HOF within agricultural fields, which have saturated hydraulic conductivity (K_s) values that are 100–200 mm h^{-1} higher. In the study area, path/furrow networks, comprising 8–24% of field surface areas, are designed to provide walking access within fields and channel excess surface flow from the fields. Compared with hoed surfaces, path/furrows reduce the time to HOF generation by about 85% and have ROCs that are six times higher. Access paths have the lowest K_s values of all watershed surfaces, but conveyance efficiency of HOF generated on these surfaces is low. Even recently created field paths are capable of reducing runoff generation time by 40–90% and producing sixfold increases in ROCs. Collectively, the data suggest that agricultural erosion rates are accelerated during the 12–18-month threshold period following abandonment and during storms where path-generated HOF interacts with adjacent planting surfaces. Despite having periods of increased HOF generation, the total HOF contribution from agricultural fields to the basin stream hydrograph is similar in magnitude to that of unpaved roads, which occupy 95% less land area. © 2001 Elsevier Science B.V. All rights reserved.

Keywords: Soil erosion; Horton overland flow; Runoff generation; Soil compaction; Infiltration; Agricultural impacts

1. Introduction

Over the last 20 years, long-term (permanent) cultivation has been replacing traditional short-term swidden practices of some ethnic hilltribe people living in mountainous northern Thailand (Schmidt-Vogt, 1998, 1999). This new intensified agricultural system has in some areas contributed to cumulative watershed effects both on-site and downstream in major river systems, such as the Chao Phraya. However, concurrent with the intensification of steep-slope agriculture has been the expansion of road systems to support national defense, law enforce-

---

* Corresponding author. Water Resources Program, EEWR, E-Quad, E-228, Princeton University, Princeton, NJ 08544, USA. Fax: +1-808-956-3512.
E-mail address: adz@princeton.edu (A.D. Ziegler).

ment, rural development, commerce, and tourism. In a prior work, we showed that the environmental impacts of unpaved roads may equal or exceed those of agricultural activities in some watersheds in northern Thailand (Ziegler et al., 2000). We also found evidence that basin footpaths and field maintenance paths act similarly to roads in enhancing the generation of Horton overland flow (HOF) in areas where it is otherwise rare. This additional runoff may accelerate erosion. Understanding the interaction of agriculture-related paths with their adjacent land surfaces is needed to fully assess the environmental impacts of any given agricultural system. In this study, we investigate runoff generation and sediment transport on three path surfaces and three agricultural surfaces within an upland watershed in northern Thailand. The research goals are to determine controls on HOF generation and to quantify the role of paths in accelerating HOF and erosion within agricultural fields.

2. Study area

All work was performed in the 93.7-ha Pang Khum Experimental Watershed (PKEW), the site of our on-going investigation of the impacts of unpaved roads in northern Thailand (Ziegler et al., 2000, 2001). Pang Khum Village (19°3′N., 98°39′E.) is within the Samoeng District of Chiang Mai Province, approximately 60 km NNW of Chiang Mai (Fig. 1), in the eastern range of the Thanon Thongchai Mountains. PKEW is part of the larger Rim River Basin, which drains into the Ping River, which in turn empties into the Chao Praya River. Bedrock is Triassic granite; PKEW soils include Ultisols, Alfisols, and Inceptisols. Roads, access paths, and dwelling sites each comprise about 1% of the PKEW area. Approximately 12% of the basin area is agricultural land (cultivated, upland fields, and < 1.5-year-old abandoned); 13%, fallow land (not used for 1.5–4 years); 31% and 12% are young (4–10 years) and advanced secondary vegetation, respectively; and 31% is disturbed, primary forest (Fig. 2).

The original pine-dominated forest has been altered by hundreds of years of swidden cultivation by Karen, Hmong, and recently, Lisu ethnic groups (Fig. 4(a)). Some attempts have been made to regenerate deforested areas by planting *Pinus kisiya* Roy ex Gord. A vegetation description is given elsewhere
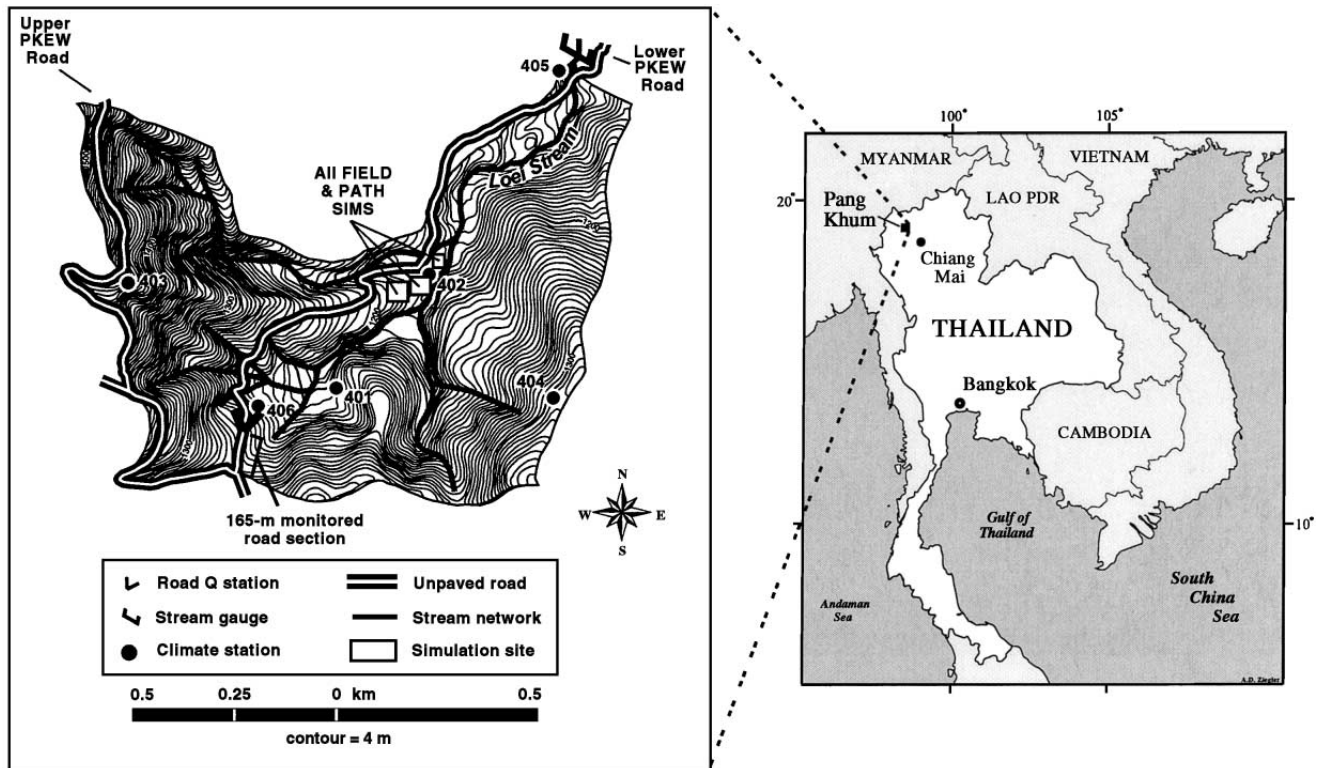

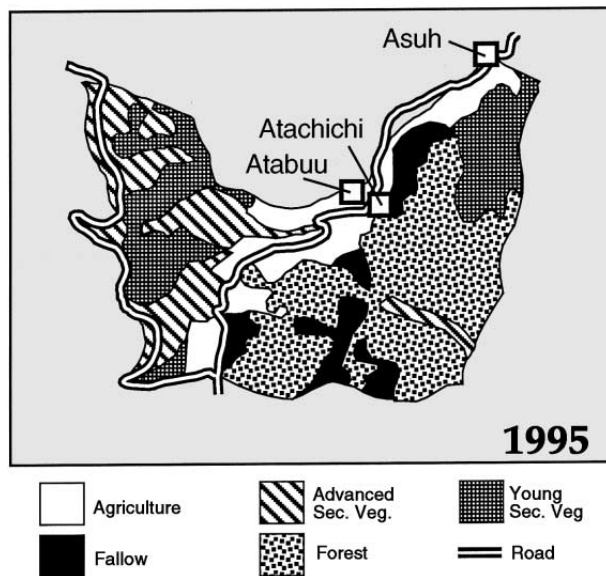Fig. 1. The 93.7-ha Pang Khum Experimental Watershed in northern Thailand.

Fig. 2. Landcover in PKEW for 1995 (based on 1:50,000 air-photos). Rectangles refer to the three Lisu fields surveyed herein.

vated crops are typically planted on sloping lands having access to irrigation. The planting surface is cleared and hoed to a depth of about 0.2 m. Organic material, including slash, is burned or pushed into ephemeral stream channels below the field. Furrow spacing is typically 1.5–2.0 m, depending on the crop and hillslope relief. These 0.1–0.2-m-deep features serve both as walking paths for field maintenance activities and conduits that channel excess surface water from the fields.

3. Methods

3.1. Compaction and infiltration indices

For simulation surfaces and other dominant land-cover surfaces in PKEW, several compaction and infiltration indices were determined. Simulation surfaces were located within a 1-ha area on a gradually sloping hillslope (Fig. 1); measurement locations for the non-simulation surfaces were spread throughout the watershed (Fig. 2). Surface bulk density (ρ_b) was determined by sampling the upper 5 cm of soil with a 90-cm^3 core, then oven drying for 24 h at 105°C. Soil penetrability, a measure of the ease an object can be pushed into the soil (cf., Bradford, 1986), was measured with a static Lang™ penetrometer (Gulf Shores, AL, USA). The penetrometer provides an index of normal strength, termed penetration resistance (PR), for the upper soil surface, typically about 0.5 cm in depth. All PR values were determined under dry soil conditions (see mass soil wetness values in Table 6). Saturated hydraulic conductivity (K_s) was estimated from infiltration mea-

(Ziegler, 2000). Most lower basin slopes are cultivated by Lisu villagers who migrated to Pang Khum from Mae Hong Son Province 20–25 years ago. The farming system now resembles a long-term cultivation system with short fallow periods, as opposed to the traditional Lisu long-fallow system (Schmidt-Vogt, 1998). Annual swidden and permanent cultivation activities, depicted in Fig. 3, are similar to those of many groups in northern Thailand (Schmidt-Vogt, 1999). Opium was a prevalent crop before government eradication began about 15 years ago. Upland rice and corn are important swidden crops; cabbage, cauliflower, onions, garlic, and flowers comprise the cultivated crops. Timing and intensity of cultivation is influenced by market demands and yearly rainfall (including the availability of irrigation water). Culti-

Permanent cultivation	limited irrigation		rainfall + irrigation					irrigation		
	harvest/prep/clearing		planting, weeding, harvesting							
Swidden	preparation	burning/planting	weeding and maintenance		harvest			prep	
Season	dry, warm	dry, hot	rainy season				rain ends	dry, cool	
Month	Feb	Mar	Apr	May	Jun	Jul	Aug	Sep	Oct	Nov	Dec	Jan

Fig. 3. Generalized calendar of annual swidden and permanent cultivation activities practiced by the Lisu in PKEW.

surements taken in situ with disk permeameters (explained in detail by Ziegler and Giambelluca, 1997). Mean slopes were determined from Abney level measurements taken every 0.25–0.5 m along a transect running through each simulation plot or along each path surface. Within three actively cultivated fields, a 400-m² subsection, chosen at random, was surveyed to determine path connectivity, path density, and path-related compaction/infiltration indices.

3.2. Rainfall simulation experiments

In the dry seasons of 1998 and 1999, four rainfall simulation experiments were performed on small-scale plots for each of the following six agricultural surfaces in PKEW: *hoed field*, *upland field*, *fallow field*, *access path*, *field path*, and *path/furrow*. Each simulation was a true replication performed on a previously untested plot. Most surfaces were created within an upland rice field that consisted of 0.25–0.50 m rice stubble. Soil surface properties of this field are shown in Table 1. Prior to simulation, the field was burned by Lisu farmers. A portion was

Table 1
Soil properties for Ap horizon (Alfisol) of the upland rice field where the rainfall simulations were performed

Property	Unit	Value
Depth	cm	15/20
Color	–	5 YR 3/2
pH	–	4.7
Sand	%	57
Silt	%	21
Clay	%	22
Dominant clay mineral	–	kaolinite
ρ_b	Mg m^{-3}	2.47
OC	%	2.52
TN	%	1.82
CEC	cmol$_c$ kg^{-1}	12.73
Ca	cmol$_c$ kg^{-1}	2.7
Mg	cmol$_c$ kg^{-1}	0.13
K	cmol$_c$ kg^{-1}	0.43
Na	cmol$_c$ kg^{-1}	0.5
% bases	%	26.4

ρ_b is bulk density; OC, organic carbon; TN, total nitrogen, CEC, cation exchange capacity.

then tilled with a traditional hand-held hoe to create the hoed field treatment. The upland field was the unhoed burned field. The 0.15-m-wide basin access path, used daily by 10–20 farmers, is the primary walking entry way into lower PKEW. The 0.14-m-wide field path surface was created by three Lisu farmers, wearing sandals, traversing up and then down a line 31 times in the hoed field (Fig. 4(b)). The path/furrow surface (Fig. 4(c)) is that which is typically dug into cultivated fields to channel water downslope and to provide walking access within the field. Fallow field consists of < 0.5-m-tall grasses and shrubs and is located about 50 m across-slope from the upland rice field. These six simulation surfaces describe the diversity of agricultural surfaces existing in the basin at any given time. Descriptions of each surface and which PKEW landuse type they represent are given in Table 2.

Simulations were performed under dry and wet soil moisture conditions. Wet simulations were conducted on the same plots, 1 day following the dry simulations. The rainfall simulator consisted of two vertical, 4.3-m risers, each directing one 60° axial full cone nozzle (70-mm orifice diameter) toward the surface. The simulator design is shown in Fig. 4(d). An operating pressure of 172 kPa (25 psi) produced rainfall energy flux densities (EFD) of 1650–2050 J m^{-2} h^{-1}, or 100–120 mm h^{-1} (note: variation in observed rainfall rates at one operating pressure was caused by wind affecting rainfall on the plot surface). This range of EFDs approximates energy sustained for 10–20 min during the largest annual PKEW storms (based on preliminary analysis of 2 years of rainfall data for stations 401 and 402, shown in Fig. 1). Cylindrical, sand-filled, low permeability geotextile bags (3.0 × 0.2 × 0.1 m) were arranged to form two side-by-side rectangular subplots. Plot dimensions for most treatments were 3.25 (L) × 0.85 (W) m; access path plots were 0.5 m longer (Table 2). At the base of each sub-plot, geotextile bags were arranged to funnel runoff into a shallow drainage trench dug into the surface. A V-shaped trough constructed from aluminum flashing was inserted into the vertical wall of the trench to allow event-based sampling. The face of the drainage trench and the triangular area below the main plot was treated with a 5:1 mixture of water and Soil Sement™ (an acrylic vinyl acetate polymer from Midwest Indus-

Fig. 4. (a) Lisu children in Pang Khum; (b) creation of the field path simulation surface by Lisu farmers; (c) the path/furrow network in Atachichi's field, 1997; (d) rainfall simulation experiment performed on the fallow field treament during 1998; (e) Ataboo's field, ca., 1999 rainy season.

trial Supply, OH, USA) to prevent sediment detachment on these nonplot areas. The sealed triangular area (an additional plot length of 0.5 m) contributed only runoff to the plot output. Rainfall rate was measured during each event with several manual gauges placed on the plot borders.

During each experiment, instantaneous discharge and sediment output were measured at time to runoff

Table 2
Description of the six simulation surfaces

Surface	Reps	Dimension (m)	Surface description	Ground cover	Surface represents
Hoed field	4	3.25 × 0.85	100% hoed	< 5%	Actively cultivated field
Upland field	4	3.25 × 0.85	100% burned upland rice field	10–20%	Upland field abandoned for 4–6 months, then burned in preparation for planting
Fallow field	4	3.25 × 0.85	100% grasses and shrubs	> 80%	Upland field unused for 16–18 months
Access path	3	3.75 × 0.85	18% path; 82% upland field	< 20%	Main walking entry path into the basin
Field path	4	3.25 × 0.85	16% path; 84% hoed field	< 5%	Newly created field maintenance path
Path/furrow	4	3.25 × 0.85	48% path/furrow; 52% hoed field	< 5%	Typical path/furrows used for walking within and channeling overland flow from fields

Paths run length-ways through the plot; path treatments combine both path and adjacent land surfaces.

(TTRO) and then at 2.5- or 5-min intervals. Discharge volume was reduced to account for presence of sediment in the samples (i.e., sampled volume minus the volume of the sediment present in the runoff sample). Instantaneous discharge and sediment output values were adjusted to rates per unit area by dividing by filling time and plot area. The rates were then divided by energy flux density (EFD) values of the simulation rainfall. Computed normalized instantaneous discharge (Q_t) and sediment output (S_t), therefore, have the units $m^3 \ J^{-1}$ and $kg \ J^{-1}$, respectively. Total normalized event discharge and sediment output, Q_{event} and S_{event}, were calculated as event total values divided by total event EFD.

4. Results

4.1. Saturated hydraulic conductivity

Of all the simulation surfaces, mean K_s is highest on the actively cultivated hoed field surface; the lowest values are on access path and path/furrow (Table 3). Upland field and fallow field values are significantly lower than the hoed field surface, indi-

cating that K_s declines over time after tilling. In general, K_s on path surfaces is much lower than on adjacent lands (Table 4). For the nonsimulation surfaces, mean K_s values on highly compacted, unpaved roads and house complex surfaces are only slightly higher than that on the access path. Surprisingly, K_s on disturbed forest, advanced secondary vegetation, and young secondary vegetation surfaces is lower than on the three tested nonpath agricultural field surfaces.

4.2. Compaction indices

Bulk density and penetration resistance data for the simulation surfaces and other PKEW landsurface types are shown in Table 3. Bulk density on access path and path/furrow surfaces are higher than on the other simulation surfaces. Road, access path, and house complex ρ_b values are the highest of all surfaces; values within the disturbed forest, the lowest. Of all the simulation treatments, fallow field has the lowest bulk density, with hoed field, upland field, and field path being only slightly higher. The PR data is in agreement with the ρ_d data in that access path, road, and house complex surfaces are the most

Table 3
Infiltration and compaction indices for simulation surfaces and other major landuse types in PKEW

	n	K_s^a (mm h^{-1})	ρ_b (Mg m^{-3})	PR (MPa)
Simulation surfaces				
Hoed field	10	347 ± 143 g	1.24 ± 0.16 d	0.6 ± 0.5 a
Upland field	6	133 ± 77 f	1.17 ± 0.06 cd	2.6 ± 1.4 b
Fallow field	12	140 ± 87 f	1.09 ± 0.05 bc	2.6 ± 1.5 b
Access path[b]	6	8 ± 5 a	1.51 ± 0.08 ef	6.7 ± 0.1 e
Field path[b]	10	244 ± 88 g	1.24 ± 0.16 d	0.7 ± 0.3 a
Path/furrow[b]	9	65 ± 25 de	1.42 ± 0.05 e	5.6 ± 0.7 de
Other land surfaces				
Forest	12	69 ± 42 cd	1.03 ± 0.07 a	3.7 ± 0.6 c
Advanced secondary vegetation	8	91 ± 38 ef	1.06 ± 0.06 ab	4.8 ± 0.6 cd
Young secondary vegetation	4	49 ± 24 cd	1.27 ± 0.04 d	4.5 ± 0.3 cd
Road	30	15 ± 8 ab	1.54 ± 0.14 f	6.6 ± 0.1 d
House	4	24 ± 12 bc	1.52 ± 0.12 ef	6.6 ± 0.1 de

[a] K_s is saturated hydraulic conductivity; ρ_b is bulk density; and PR is penetration resistance; means are ±1 standard deviation; values with the same letter in a column are NOT statistically distinguishable using one-way analysis of variance (ANOVA) on $\log_{10}$-transformation data followed by post-hoc multiple comparison testing with the Fisher's protected least squares difference test when the F-values were significant at $\alpha = 0.05$.

[b] Values were determined on the path portion of the simulation plot.

Table 4

Relative percent change between compacted path surface and adjacent agricultural surface compaction, infiltration, and runoff variables

Path surface: Agricultural surface	ρ_b^a	PR	K_s	$TTRO_{dry}$	$TTRO_{wet}$
Access path: upland field	25	158	−94	−80[b]	−35
Access path: fallow field	36	158	−94	−80[b]	−98[b]
Path/furrow: hoed field	17	833	−81	−85[b]	−90
Field path: hoed field	0	17	−30	−43[b]	−95

[a] ρ_b is bulk density; PR is penetration resistance; K_s is saturated hydraulic conductivity; TTRO is time to runoff under dry or wet simulation conditions.

[b] Owing to no runoff after 60-min simulation time, these differences are minimal values.

compacted. In contrast to the bulk density data, however, the PR values for the field path and hoed path are significantly lower than all other surfaces; and young/advanced secondary values were higher than those of upland field and fallow field. Table 5 shows on- and off-path bulk density values determined in the three actively cultivated fields shown in Fig. 2. Path ρ_b is significantly higher than that on the field growing surface (Mann–Whitney U-test, $\alpha = 0.05$) for all three fields.

4.3. Rainfall simulation runoff and sediment transport data

Rainfall simulation results are shown in Table 6. For both dry and wet antecedent moisture conditions,

no runoff was produced on fallow field after 60 min of simulated rainfall. During the dry simulations, access path generated runoff in half the time as upland field and had a 50% higher runoff coefficient (ROC, ratio of total runoff to total rainfall). For wetter conditions, TTRO, Q_{event}, and ROC for these two surfaces are nearly identical. The sediment transport data for these two surfaces are also indistinguishable. Within the cultivated field, path/furrow and field path generated runoff sooner during both dry and wet conditions than did hoed field, which required more than 60 and 30 min, respectively, to produce runoff during the two simulation suites. Owing to limited HOF on the hoed surface, sediment transport was minimal, as compared with the path/furrow and field path surfaces. Because the slope of the path/furrow simulation was approximately half that of the other treatments, observed runoff and sediment transport values are probably conservative.

Normalized instantaneous discharge (Q_t) and sediment transport (S_t) for all six surfaces tested during rainfall simulation are shown in Fig. 5. Question marks indicate uncertainty in TTRO for hoed field (HF) and fallow field (FF), as described above. Response curves for each surface are manually smoothed through corresponding time series to show general trends in Q_t and S_t. Of note are (i) unique TTRO values for all treatments under dry antecedent moisture conditions; (ii) similarity between upland field (UF), access path (AP), field path (FP), and path/furrow (P/F) discharge during the wet simulations; and (iii) susceptibility of the field path treat-

Table 5

On-path and off-path bulk density, slope, and area-related variables for the cultivated fields shown in Fig. 2

Field	Number[a] of paths	Slope (°)	$\rho_{b\,(on\text{-}path)}$ (Mg m^{-3})	$\rho_{d\,(off\text{-}path)}$ (Mg m^{-3})	Width (m)	Path density (m m^{-2})	Path area (%)
Atabuu	19	18.3 ± 6.1 (78)[b]	1.25 ± 0.07 (10)	1.10 ± 0.05 (10)	0.24 ± 0.04 (78)	0.41	11
Asuh	16	15.5 ± 8.9 (54)	1.19 ± 0.06 (10)	0.98 ± 0.09 (10)	0.25 ± 0.05 (54)	0.33	8
Atachichi	23	6.4 ± 1.0 (36)	1.42 ± 0.05 (10)	1.19 ± 0.07 (10)	0.41 ± 0.04 (36)	0.58	24

[a] Paths are the number of paths per 400-m^2 sampled area; ρ_d is bulk density of the path or cultivated field surface; path density is path length divided by field area; path area is path area divided by field area.

[b] Values are means $\pm$ standard deviations; values in parentheses are sample sizes; all on-path ρ_b values are significantly higher than corresponding off-path values (Mann–Whitney U-test, $\alpha = 0.05$).

Table 6
Runoff and sediment data for the six rainfall simulation treatments

Treatment	Slope (°)	w^a (g g^{-1})	Dry conditions					Wet conditions					
			EFD (J m^{-2} h^{-1})	TTRO (min)	Q_{event} (1 J^{-1})	ROC (%)	S_{event} (g J^{-1})	w (g g^{-1})	EFD (J m^{-2} h^{-1})	TTRO (min)	Q_{event} (1 J^{-1})	ROC (%)	S_{event} (g J^{-1})
Hoed field[b]	13	0.06	1753	>60	–	–	–	0.27	1898	31.3	0.002	0.04	0.02
Upland field	13	0.04	1796	26.5	0.07	0.12	0.04	0.24	2320	2.0	0.022	0.40	0.13
Fallow field	18	0.04	1634	>60	–	–	–	0.35	1748	>60	–	–	–
Access path	12	0.05	1849	12.1	0.010	0.18	0.06	0.22	2042	1.3	0.022	0.38	0.11
Field path	12	0.06	1807	34.1	0.004	0.06	0.14	0.28	2046	1.6	0.014	0.26	0.52
Path/furrow	6	0.02	1641	9.0	0.006	0.11	0.02	0.26	1754	3.0	0.014	0.24	0.07

Dash indicates no data because runoff was not initiated after 40 min of simulation.

[a] w is antecedent mass wetness; EFD is energy flux density of the simulated rainfall; TTRO is time to runoff; Q_{event} is normalized event discharge; S_{event} is normalized total event sediment transport.

[b] $n = 4$ for all treatments except access path ($n = 3$); dry simulations were carried out for 60 min after TTRO; wet simulations, 30 min after TTRO.
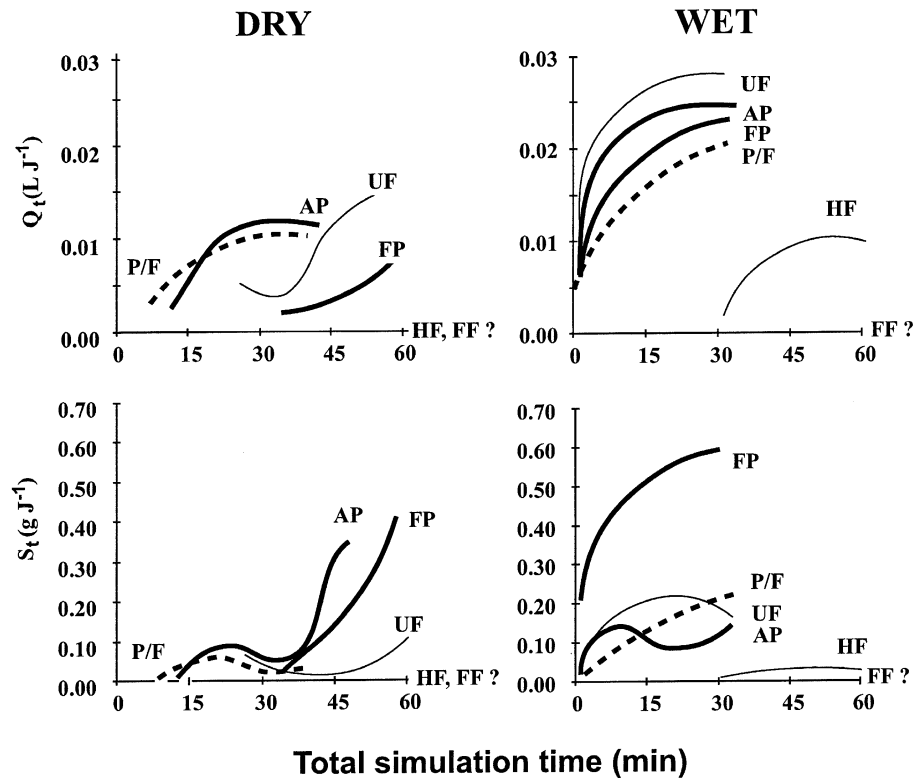
Fig. 5. Instantaneous discharge (Q_t) and sediment transport (S_t) for the six simulation surfaces during the dry and wet simulations. The surfaces are hoed field (HF), upland field (UF), fallow field (FF), access path (AP), field path (FP), and path/furrow (P/F).

ment to surface erosion once sufficient runoff is generated, as compared with that on the hoed field.

5. Discussion

5.1. Temporal variation in overland flow

Both actively cultivated fields and fields that have been abandoned for at least 16–18 months (i.e., fallow field) require a high threshold rainfall depth before producing HOF. Hoeing maintains a rough, porous surface on cultivated fields during the extended growing season. Infiltrability on this surface horizon, as indicated by the K_s data, is the highest of all surfaces measured in PKEW. Horton flow is rare on fallow surfaces older than about 16–18 months, in part, because of moderately high K_s, but more importantly, because the dense vegetation cover both intercepts rainfall and ponds surface water. Comparison of hydrologic response data (i.e., TTRO, Q_{event}, and ROC) from hoed field, upland field, and fallow field simulations suggests the existence of a

threshold period, lasting from the end of harvest until the time when dense vegetative cover is established, during which HOF is generated by lower threshold rainfall depths. Similarly, Chandler and Walter (1998) found pasture-fallow lands to have the lowest rainfall thresholds for HOF generation on several agricultural surfaces in an upland area in the Philippines. Similarity in K_s between upland field and fallow field indicates that the enhanced HOF generation capability on the recently abandoned upland field results from vegetative cover being insufficient to (i) pond water and impede surface flow or (ii) retard raindrop impact, which may contribute to surface sealing. It is plausible that, in the absence of field paths, annual erosion rates on agricultural lands in PKEW are highest during this transition period where HOF generation is most likely.

5.2. Role of paths in accelerating Horton overland flow

Path surface infiltrability is less than on most surrounding nonpath lands because compaction from

walking has destroyed soil aggregates, reduced macroporosity, and sealed the surface, thereby reducing surface K_s. Our ρ_b and PR data in PKEW show all path surfaces to be more compacted than the surrounding agricultural surfaces. Table 4 shows 17–36% increases in ρ_b and 158–833% increases in PR for path versus agricultural surfaces. These increases in compaction indices result in 81–94% decreases in K_s. With regard to the undetectable ρ_b increase on the field path simulation surface, the 31 passes compacted a very shallow surface layer (e.g., PR increased 17%) but did not affect ρ_b when integrated over a depth of 5 cm. The shallow compaction, however, was enough to decrease K_s by 38%, demonstrating that relatively minor human activity in cultivated fields can initiate changes in infiltrability. In comparison with our PKEW compaction and K_s data, other studies have similarly found 73–100% decreases in infiltration rate, 6–100% increases in ρ_b, and 90–800% increases in PR (various measurement devices) to result from hiking, trampling, or camping activities (Weaver et al., 1979; Shoba and Sokolov, 1982; Cole, 1986; Jim, 1987a,b; Harden, 1992; Stewart and Cameron, 1992; Sun and Liddle, 1993; Wallin and Harden, 1996; Sutherland et al., submitted). The 13–20% difference between path and off-path ρ_b in the three surveyed fields indicates that paths undoubtedly enhance in-field HOF generation (Table 5).

Time to runoff on the access path was at least 35–80% faster than for the two agricultural surfaces, upland field and fallow field, during rainfall simulations (Tables 4 and 6). Within the cultivated field, where path/furrow K_s was 81% lower than that of hoed field, TTRO occurred at least 85% sooner on this compacted surface than on the hoed surface during both dry and wet simulations. Similarly, the newly created field path surface greatly reduced TTRO on the hoed surface, particularly during wet antecedent moisture conditions where runoff was generated 95% faster. On this moderately compacted path surface, rain-affected flow processes during rainfall simulations may have further dispersed fine material into surface pores, creating a smooth, sealed surface that initiated HOF in < 2 min during the wet simulations. In general, the path-related surfaces had higher event ROCs than the adjacent nonpath agricultural surfaces (Table 6). For example, the field

path wet simulation ROC was six times higher than that for hoed field. In comparison, during a study in Costa Rica, Wallin and Harden (1996) determined path ROC values to be 12–40 times greater than off-path ROCs. In an earlier study, Harden (1992) found on-path ROCs to range from 51% to 59%. As an exception, access path and upland field values were similar during the wet simulations, demonstrating that the abandoned surface had insufficient vegetation cover to intercept rainfall, store surface water, and impede surface flow. Our path simulation values appear to be lower than those of these other two studies; however, ours are for plot surfaces combining path and adjacent land surfaces. In sum, our simulations collectively show that the compacted path surfaces enhance HOF generation on their host surfaces.

5.3. Path density

Path-related increases in HOF can be important if path densities are high and path-related runoff is conveyed efficiently to the stream system. Much of the access path exists within lands having relatively high K_s values, i.e., on disturbed forest, secondary vegetation, upland field, and fallow field surfaces (Table 3). Distance between the path and the stream network is typically > 50 m (field observations; airphoto interpretation)—a distance great enough for most on-path HOF exiting on to the hillslope to be infiltrated before reaching the stream. Through observation during two rainy seasons, we generally believe the conveyance efficiency for HOF generated on basin access paths to be low in PKEW, except where the paths descend directly to the stream network (about 5–10% of the total basin path length). While the primary access path is a permanent PKEW feature, the whole network of field access paths expands and contracts in response to basin farming, forestry, and gathering use. Thus, our 1998 access path length estimate of 6130 m could vary by approximately ±25% during any given year. Footpaths accessing remote fields may be utilized sparingly for only a few months during a several-year period. When used infrequently, the paths become overgrown with grasses, shrubs, and tree seedlings, which quickly reduce HOF generation on the compacted surface by increasing interception and surface water

storage, despite in situ K_s remaining relatively low for a longer period. However, tilling or hoeing for cultivation probably restores the infiltrability of the path surface immediately, if compaction is not too deep (cf., Luce, 1997).

Within cultivated fields, path drainage densities ranged from roughly 0.3 to 0.6 m m^{-2} (Table 5). The 23 path/furrows in the 400-m^2 surveyed section of Atachichi's field comprise 24% of the total field area (Fig. 4(c)). In comparison, the 16 and 19 path/furrows within two other fields comprise only 8% and 11% of the total surface area, respectively. Within Atabuu's field (Figs. 4(e) and 6), mean path slope exceeds 15°; and average path length is 10 m. Because of high connectivity of the path/furrow network, these relatively long, steep features can generate HOF capable of incising the path surface or eroding the adjacent planting surface. Although the path/furrows are initially 0.1–0.2 m below the planting surface, the borders become less distinct over the course of the growing season. For large storms, where sufficient HOF is generated (e.g.,
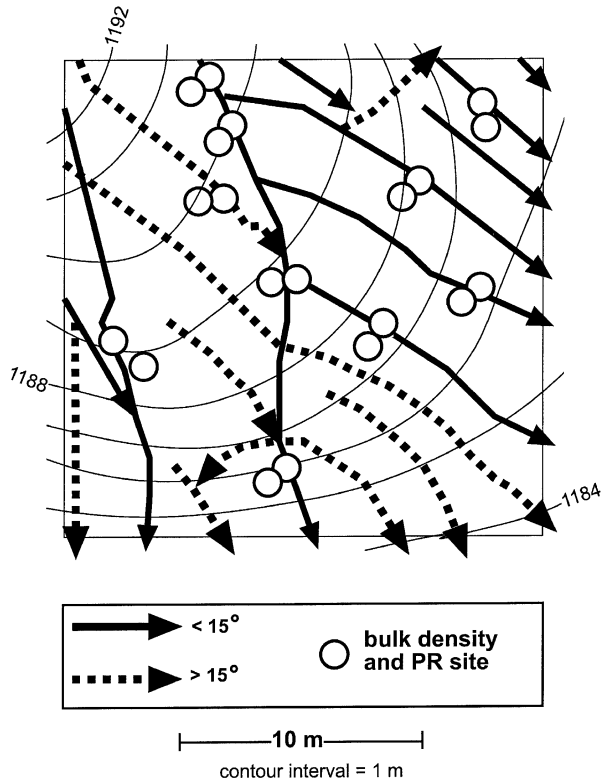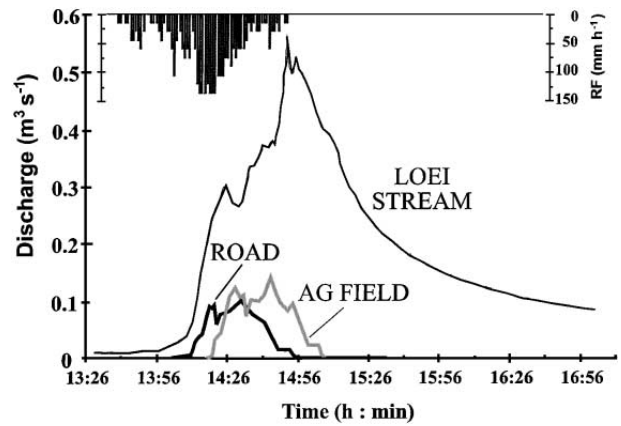

Fig. 7. The HOF contribution of roads and agricultural surfaces to the Loei stream storm hydrograph during *storm*. AG field was represented by the following simulation surfaces: 15% upland field (UF), 42.5% hoed field (HF), and 42.5% hoed field + path/furrow (area weighted to match the path densities in PKEW). Total AG field area in PKEW is 12%.

storm discussed below), runoff water leaving a path/furrow erodes the planting surface before being channeled back into a downslope furrow or exiting onto the hillslope below. The field path simulations show the susceptibility of the hoed planting surface to sediment transport when sufficient HOF is generated. It is therefore likely that erosion within cultivated fields is high in PKEW when path-generated HOF detaches and entrains material from the planting surface. This phenomenon has also been observed in other areas of northern Thailand, e.g., Mae Sa Mai and Pakha (F. Turkelboom, Soil Science Department, K.U. Leuven, Belgium, personal communication).

5.4. Field path contribution to basin runoff: an example

Fig. 7 shows the estimated HOF contributions from roads and agricultural fields (AG fields) to the Loei stream hydrograph during the largest event in 1998 (Aug 15, referred to as *storm*). During the 30-min period of the highest rainfall, mean 1-min intensity (89 mm h^{-1}) for *storm* is only slightly lower than the rainfall simulation mean (105 mm h^{-1}). *Storm* EFD, however, is substantially higher (2640 versus 1775 J m^{-2} h^{-1}) because median PKEW raindrop size is 50% larger than that for

Fig. 6. Generalization of the path/furrow network in Atabuu's field. Circles indicate sites of bulk density measurements.

simulated rainfall (Baruah, 1973; Ziegler et al., 2000). Stream discharge is recorded at a gauging station located at the mouth of the basin (Fig. 1). The road-generated HOF contribution to streamflow is calculated as

$$Q_{i,\text{HOF}}$$
$$= \text{Area}_{\text{ROAD}} * \text{CE}_{\text{ROAD}} * \text{EFD}_{i,\text{STORM}} * q_{i,\text{ROAD}}$$

(1)

where $\text{Area}_{\text{ROAD}}$ $[\text{m}^2]$ is the area of the PKEW road network; CE_{ROAD} is the conveyance efficiency of road runoff to the stream channels (approximately 70%; Ziegler et al., 2001); $\text{EFD}_{i,\text{STORM}}$ is the energy flux density $[\text{J m}^{-2} \text{ h}^{-1}]$ of *storm* (calculations described by Ziegler et al., 2000); and $q_{i,\text{ROAD}}$ is the mean energy-normalized instantaneous runoff $[\text{m}^3 \text{ J}^{-1}]$ determined during a suite of prior road rainfall simulations in PKEW (Ziegler et al., 2000).

The HOF contribution of AG fields to streamflow was calculated with Eq. (1), using simulation data determined herein and a basin agricultural area of 12%. Fifteen percent of the AG field was assumed to be composed of surfaces similar to upland field; the remaining 85% was equally divided as path/furrow and hoed field (1998 field survey). A simple delay, extrapolated from small-scale rainfall simulation data, was applied to the rising and falling limbs of the road and AG field HOF hydrographs. Conveyance efficiency for both AG field surfaces was assumed to be 100%. Surface runoff from saturation overland flow is ignored. Although not a precise hydrograph separation—because the conveyance efficiency was a maximal estimate—the AG field estimate illustrates HOF-based streamflow contribution from agricultural lands during large events is likely on the
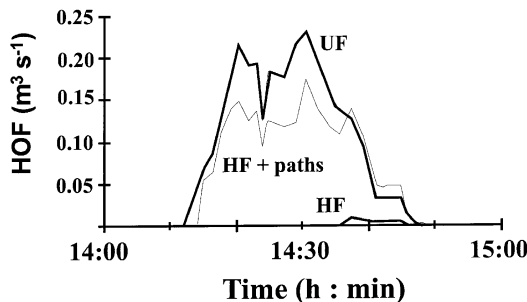

Fig. 8. The relative contribution of three agricultural surfaces to AG field HOF during *storm*. Surface areas are described in Fig. 7 caption.

Table 7
Predicted runoff and sediment transport from three fields during *storm*

Field	Area (cm^2)	Cultivated		Cultivated + path/furrows	
		Q (m^3)	S (kg)	Q (m^3)	S (kg)
Atabuu	664	1.0	19.2	2.6	30.2
Asuh	1000	1.4	27.1	3.2	38.4
Atachichi	900	1.3	16.1	6.1	36.3

Cultivated values are based on the hoed simulation data; cultivated + path/furrows values are area-weighted calculations based on hoed and path/furrow simulation data.

same order of magnitude as that for roads, for which HOF comprised approximately 10% of the basin hydrograph during the first 1–2 h after the storm initiation. For smaller events, road contributions would likely increase because of the relatively low threshold rainfall depths needed to generate HOF on these highly compacted surfaces, with low K_s, as compared with agricultural surfaces. In an earlier work, we hypothesized that roads contribute to basin runoff hydrographs disproportionately to their areal extents (Ziegler and Giambelluca, 1997), which in PKEW is less than 5% that of the AG field. Fig. 8 shows HOF generated on the three agricultural surfaces comprising AG field during *storm*. This comparison shows the limited HOF generated on actively cultivated fields, even during large seasonal events, as *storm* was one of a few events in the 2-year data set with a rainfall depth high enough to generate HOF on the hoed field surface. It also shows the ability of paths and furrows to boost HOF generation on cultivated surfaces, if path-contributing areas are sufficient.

Table 7 compares predicted runoff and sediment transport on three fields during *storm*, for two landuse scenarios: (i) 100% hoed field and (ii) a combination of hoed field and path/furrow. Values are calculated using rainfall simulation Q_{event} and S_{event}, *storm* EFD, and corresponding areas for the three fields. Conveyance efficiencies are equal to simulation ROCs. For the scenario combining hoed field and path/furrows, simulation data was area-weighted to match path densities found in each field. For fields steeper than the rainfall simulation surfaces, sediment transport was increased using the WEPP slope

factor (Flanagan and Nearing, 1995). Collectively, these estimates shown in Table 7 demonstrate the potential for the path/furrow network to increase field erosion by 40–125% for storms with magnitude similar to that of *storm*. The sediment transport estimates are probably low because they do not account for sediment transport related to overland flow running onto the hoed surface from upslope path/furrows as discussed above. The actual values will also depend on the conveyance efficiency of overland flow from the field, which, owing to the high connectivity of the path/furrow network in PKEW, are potentially as high as the estimates we used.

5.5. Final note: saturated hydraulic conductivity in PKEW

In a prior work (Ziegler and Giambelluca, 1997), we reported substantially different mean K_s values for roads (2.3 mm h^{-1}, $n = 18$), agricultural/secondary vegetation (105 mm h^{-1}, $n = 22$), and forests (524 mm h^{-1}, $n = 11$) in two areas of northern Thailand, Kae Noi and Pang Khum (referred to as Sam Mun in the earlier paper). Most of the prior values were determined with the same disk permeameters and measurement methodology used in this study. Discrepancies, therefore, are likely related to incorporating values measured outside of PKEW. For example, all but five road K_s values were determined in Kae Noi; and the Pang Khum values were all collected outside PKEW. The K_s values taken on PKEW agricultural lands that comprise the agricultural/secondary vegetation category have a mean of approximately 150 mm h^{-1}, which is in line with that of upland field and fallow field. The highest PKEW agricultural K_s values in the prior study (150–230 mm h^{-1}) were taken on cultivated fields. All of the prior forest values were taken outside of PKEW, probably within forests that are less degraded than those in PKEW. The low forest values in this data set may by an artifact of our sampling methodology. Most forested areas in PKEW were excluded from testing because they occur on steep slopes, where use of the permeameters would have required disturbing the surface by leveling. Thus, many forest K_s measurement sites were likely disturbed by human/animal trampling, which consoli-

dates the surface, thereby reducing K_s. Current work is directed toward verifying our forest K_s estimates.

6. Summary

Horton overland flow is rare on actively cultivated fields and fallow fields that have been abandoned for a long enough period of time to establish a vegetative cover capable of intercepting rainfall, ponding surface water, and increasing soil infiltrability. For a transition period of about 12–18 months following abandonment, fallow fields have a greater potential to generate HOF and accelerate sediment transport than during the previous cultivated period or the following advanced fallow period. Owing to diminished K_s, walking paths and field maintenance paths (and/or furrows) generate HOF on agricultural lands where this type of runoff is otherwise rare. Thus, for the largest seasonal storms, paths potentially accelerate agricultural erosion by an estimated 40–125% in fields where paths cover 11–24% of the total area. Basin access path density expands and contracts seasonally in response to human usage of remote fields in the watershed. Regardless of the nature of agricultural lands to pass through periods where the potential for HOF is enhanced, and irrespective of the ability of paths to boost HOF generation, the maximum basin runoff attributed to HOF on agricultural related lands in PKEW is probably only on the same order of magnitude as that generated on the road network, which occupies about 95% less area. This initial conclusion is offered without our being able to precisely quantify the conveyance efficiency of runoff from agricultural lands to the stream network. Future work is directed at improving these estimates. Additionally, we have not yet determined what are critical path densities for which HOF generated on the path network significantly accelerates in-field erosion rates. Fully understanding the relative impacts of roads versus agricultural activities in PKEW will require advancement in these two areas.

Acknowledgements

References

Baruah, P.C., 1973. An investigation of drop size distribution of rainfall in Thailand. PhD Dissertation, Asian Institute of Technology, Bangkok, Thailand.

Bradford, J.M., 1986. Penetrability. In: Klute, A. (Ed.), Methods of Soil Analysis: Part 1. Physical and Mineralogical Methods, Agronomy Monograph No. 9. 2nd edn. American Society of Agronomy–Soil Science Society of America, Madison, WI, pp. 463–478.

Chandler, D.G., Walter, M.F., 1998. Runoff responses among common land uses in the uplands of Matalom, Leyte, Philippines. Am. Soc. Agric. Eng. Trans. 41 (6), 1635–1641.

Cole, D.N., 1986. Recreational impacts on backcountry campsites in Grand Canyon National Park, Arizona, USA. Environ. Manage. 10 (5), 651–659.

Flanagan, D.C., Nearing, M.A., 1995. USDA-Water Erosion Prediction Project: Technical Documentation. NSERL Rep. No. 10. National Soil Erosion Res. Lab, West Lafayette, IN.

Harden, C.P., 1992. Incorporating roads and footpaths in watershed-scale hydrologic and soil erosion models. Phys. Geogr. 13 (4), 368–385.

Jim, C.Y., 1987a. Camping impacts on vegetation and soil in a Hong Kong country park. Appl. Geogr. 7, 317–332.

Jim, C.Y., 1987b. Trampling impacts of recreationists on picnic sites in a Hong Kong country park. Environ. Conserv. 14 (2), 117–127.

Luce, C.H., 1997. Effectiveness of road ripping in restoring infiltration capacity of forest roads. Restor. Ecol. 5 (3), 256–270.

Schmidt-Vogt, D., 1998. Defining degradation: the impacts of swidden on forests in northern Thailand. Mt. Res. Dev. 18 (2), 135–149.

Schmidt-Vogt, D., 1999. Swidden farming and fallow vegetation in northern Thailand. Geoecological Research, vol. 8, Franz Steiner Verland, Stuttgart, Germany, 342 pp.

Shoba, S.A., Sokolov, L.A., 1982. Changes in the microfabric of sod-podzolic soils in recreational load zones. Sov. Soil Sci. 14, 85–91.

Stewart, D.P.C., Cameron, K.C., 1992. Effect of trampling on the soils of the St. James Walkway, New Zealand. Soil Use Manage. 8 (1), 30–36.

Sun, D., Liddle, M.J., 1993. A survey of trampling effects on vegetation and soil in eight tropical and subtropical sites. Environ. Manage. 17 (4), 497–510.

Sutherland, R.A., Bussen, J.O., Plonke, D.L., Evans, B.M., Ziegler, A.D., submitted. Hydro-physical degradation associated with hiking trail use: a case study of Hawai'iloa Ridge Trail, O'ahu, Hawai'i. Land Degrad. Devel.

Wallin, T.R., Harden, C.P., 1996. Estimating trail-related soil erosion in the humid tropics: Jatun Sacha, Ecuador, and La Selva, Costa Rica. Ambio 25 (8), 517–522.

Weaver, T., Dale, D., Hartley, E., 1979. The relationship of trail condition to use, vegetation, user, slope, season and time. In: Ittner, R., Potter, D.R., Agee, J.K., Anschell, S. (Eds.), Recreational Impact on Wildlands. Conference Proceedings, US Forest Service No. R-6-001-1979, Seattle, WA.

Ziegler, A.D., 2000. Toward modeling road erosion in northern Thailand. PhD Dissertation, Geography Dept., University of Hawaii, Honolulu, 105 pp.

Ziegler, A.D., Giambelluca, T.W., 1997. Importance of rural roads as source areas for runoff in mountainous areas of northern Thailand. J. Hydrol. 196 (1/4), 204–229.

Ziegler, A.D., Sutherland, R.A., Giambelluca, T.W., 2000. Runoff generation and sediment transport on unpaved roads, paths, and agricultural land surfaces in northern Thailand. Earth Surf. Processes Landforms 25 (5), 519–534.

Ziegler, A.D., Sutherland, R.A., Giambelluca, T.W., 2001. Interstorm surface preparation and sediment detachment by vehicle traffic on unpaved mountain roads. Earth Surf. Processes Landforms 26 (3), 235–250.